JACS
JOURNAL OF THE AMERICAN CHEMICAL SOCIETY
Article
pubs.acs.org/JACS

Dual-Site Fluorescent Probe for Visualizing the Metabolism of Cys in Living Cells

Yongkang Yue,[†,§] Fangjun Huo,[‡,§] Peng Ning,[∥] Yongbin Zhang,[‡] Jianbin Chao,[‡] Xiangming Meng,*[,∥] and Caixia Yin*[,†]

[†]Key Laboratory of Chemical Biology and Molecular Engineering of Ministry of Education, Key Laboratory of Materials for Energy Conversion and Storage of Shanxi Province, Institute of Molecular Science, Shanxi University, Taiyuan 030006, China

[‡]Research Institute of Applied Chemistry, Shanxi University, Taiyuan 030006, China

[∥]Department of Chemistry, Anhui University, Hefei 230601, China

Supporting Information

ABSTRACT: Fluorescent probes, as noninvasive tools for visualizing the metabolism of biomolecules, hold great potential to explore their physiological and pathological processes. For cysteine (Cys), however, none of the reported fluorescent probes could image the metabolic processes in living cells. To achieve this goal, we developed a coumarin derivative based on rational design of the dual recognition sites for Cys and its metabolite, SO_2. The probe displayed distinct two channels with turn-on fluorescent emission toward Cys and SO_2, which were successfully applied for imaging both A549 cells and zebrafish. Further, with reversible fluorescent responses toward Cys, the probe could image the enzymatic conversion of Cys to SO_2 in living A549 cells in a ratiometric manner. The present work reports the first probe to image the endogenous generated SO_2 without incubation of the SO_2 donors.

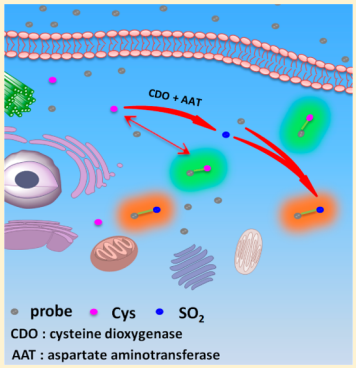

INTRODUCTION

Cysteine (Cys) is one of the sulfhydryl-containing small-molecular amino acids that play crucial roles in many physiological and pathological processes. In biological systems, Cys is generated primarily from methionine by methionine-adenosyltransferase, adenosylhomocysteinase, cystathionine-β-synthase, and cystathionine-γ-lyase. Further, for the consumption of Cys, cysteine dioxygenase, which exists in almost all mammalian cells except erythrocytes, catalyzes cysteine to cysteinesulfinate and further converts to β-sulfinylpyruvate enzymatically by aspartate aminotransferase, and then decomposes to pyruvate and SO_2, which exist at equilibrium as HSO_3^- and SO_3^{2-} in biological environments, spontaneously.[1] Normal levels of Cys (30−200 μM) maintain the synthesis of various proteins and the main antioxidant glutathione (GSH), and act as the source of sulfide in human metabolism.[2] Excess amounts of Cys, however, are associated with diseases including rheumatoid arthritis, Parkinson's disease, and Alzheimer's disease.[3] On the other side, a deficiency of Cys is reported to cause slowed growth, edema, liver damage, skin lesions, and weakness.[4] Thus, it is critically important to visualize the metabolism of the endogenous homeostasis of Cys. For this, many existing thiol fluorescent probes have been broadly used, such as determining Cys concentration from serum or proteins and cell imaging of the replenishment of intracellular cysteine. However, to our knowledge, none of them has realized the monitoring of the metabolic processes of Cys, which is essential to gain deeper insight into the physiological and pathological roles of Cys.[5]

In this respect, fluorescent probes to visualize the metabolic processes of Cys should meet at least three prerequisites: (a) the reaction between the probe and Cys should be reversible,[6] (b) the fluorescence responses of the probe toward the metabolite (such as SO_2) of Cys should be distinct with the probe−Cys system, and (c) both of the reaction processes should be fast to promote real-time imaging. With these criteria in mind, we selected α,β-unsaturated ethanoylcoumarin as the fluorophore and the thiols reaction site, which may feature reversible responses toward thiols with the addition of *N*-ethylmaleimide (NEM), a thiol-scavenging reagent.[7] Coumarin dyes have been widely used in designing low-toxicity fluorescent probes with excellent fluorescence properties which would benefit their biological applications.[1e,8] Further, the benzaldehyde moiety is known to be a sensitive reaction site for SO_2 through nucleophilic addition.[8e,9] Combining ethanoylcoumarin with terephthalaldehyde, we develop **1** (Scheme 1 and Scheme S1) as the designed fluorescent probe to visualize the metabolism of Cys in living cells. As expected, the dual-site probe **1** can discriminatively detect thiols and sulfite through two emission channels with fast responses. Cell and zebrafish imaging experiments demonstrate the application of **1** as an appealing bioimaging probe. Further, as

Received: December 17, 2016
Published: February 7, 2017

DOI: 10.1021/jacs.6b12845
J. Am. Chem. Soc. 2017, 139, 3181−3185

Scheme 1. (a) Aerobic Metabolism of Cys in Mammalian Cells and (b) Design of the Dual-Site Fluorescent Probe for Cys Metabolism Visualization

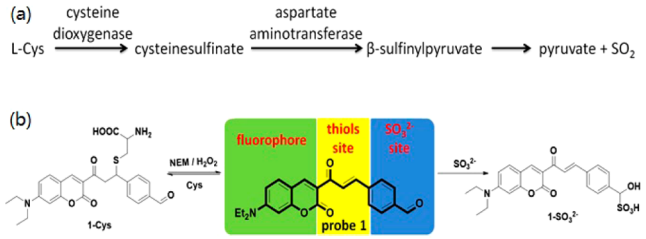

far as we know, **1** is the first reported probe to image the endogenous generated sulfur dioxide derivatives without incubation of the SO_2 donors such as $Na_2S_2O_3$ and 2,4-dinitrobenzenesulfonamide.[1e,10]

RESULTS AND DISCUSSION

Fluorescent Responses of Probe 1 to Cys. The UV−vis and fluorescent responses of **1** toward Cys were first measured systematically upon gradual addition of Cys over a concentration range of 0−400 μM to **1** in PBS/DMSO (1/1, v/v, pH 7.4). As shown in Figure 1a, **1** displayed nonfluorescent

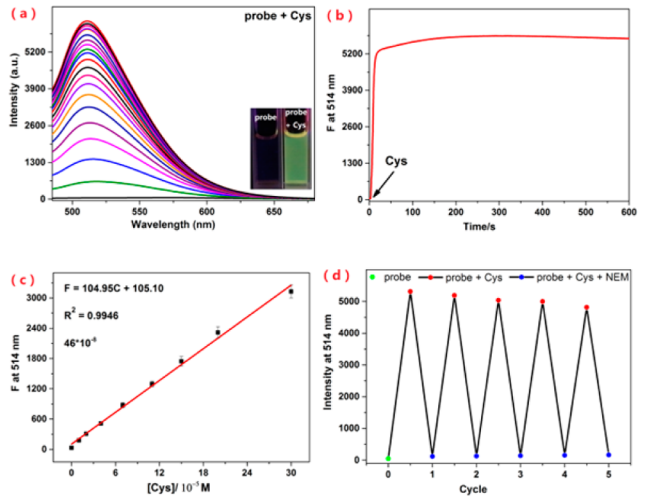

Figure 1. (a) Fluorescent response of 20 μM probe **1** upon addition of 400 μM Cys in PBS/DMSO (1/1, v/v, pH 7.4) system. Inset: corresponding fluorescent color change under the irradiation of a hand-held UV lamp. (b) Time-dependent fluorescent emission of the 20 μM probe **1** and 400 μM Cys system at 514 nm. (c) Working curve of **1** to detect Cys obtained by addition of various concentrations of Cys (0−300 μM) to 20 μM probe **1**. (d) Reversibility study of **1** (20 μM) toward Cys (400 μM) upon addition of NEM (400 μM). λ_{ex} = 463 nm; slit, 5 nm/5 nm.

emission in the above system; however, the addition of Cys induced a turn-on fluorescence emission at 514 nm and peaked with a 130-fold enhancement. Accompanying the fluorescence changes, the maximum absorption peak in the UV−vis spectra changed from 475 to 450 nm (Figure S1). The time-dependent fluorescent response (Figure 1b) of **1** toward Cys (1 equiv probe **1**:20 equiv Cys) at 514 nm displayed that the detection process balanced within 100 s, and so the subsequent fluorescent data were all measured 2 min after the addition of analyte. The corresponding detection limit based on the IUPAC definition (CDL = 3 Sb/m) was 0.46 μM from 10 blank solutions (Figure 1c). Notably, the fluorescent emission of Cys-added **1**-containing system could effectively be quenched by the addition of NEM and then restored by further addition of Cys (Figure 1d). The reversible cycling determinations—namely, five times supplement of Cys and subsequent NEM—were carried out with negligible intensity attenuation, which indicated that **1** might be used as an efficient tool for real-time measurement of the Cys concentrations in vitro and in vivo.

To evaluate the effect of various analytes, including amino acids, intracellular nucleophiles, and H_2O_2, on probe **1**, a 400 μM concentration each of Ala, Asn, Arg, Asp, Gln, Glu, Gly, His, Ile, Leu, Lys, Met, Phe, Pro, Ser, Thr, Trp, Tyr, Val, SH^-, SO_3^{2-}, and H_2O_2 was added to a system of **1** in PBS/DMSO (1/1, v/v, pH 7.4). None of them could induce a distinct fluorescent enhancement at 514 nm (λ_{ex} = 463 nm) (Figure S2). For the sulfhydryl-containing amino acids, 400 μM homocysteine (Hcy) induced almost the same fluorescent responses as 400 μM Cys (Figure S3). Considering the physiological level of homocysteine (5−13 μM), the interference induced by Hcy was negligible in the detection system.[6,11] Besides, the reaction of probe **1** with 1 mM GSH was hyperslow. Thus, probe **1** could detect Cys with relatively high selectivity. Further, the pH effect was measured upon addition of 400 μM Cys into 20 μM **1** in a mixture of DMSO/PBS (1/1, v/v) with pH changing from 3 to 12 (Figure S4). The spectra displayed that all there was strong emission at 514 nm with a 463 nm excitation in the range of pH 5−11. The results obtained showed that detection could be realized over a broad pH range.

Prompted by the inertness of probe **1** toward H_2O_2, we wondered whether the fluorescence of the Cys−probe **1** system could be quenched by the addition of H_2O_2, which could consume Cys to form cystine.[12] As shown in Figure S5, H_2O_2 addition into a probe **1**−Cys balanced system in PBS/DMSO (1/1, v/v, pH 7.4) induced a distinct fluorescence intensity decrease and eventually quenched it within 12 min at 514 nm. Upon addition of more Cys to the quenched system, the fluorescence recovered dramatically (Figure S6). Considering the antioxidant nature of Cys, probe **1** might be used to monitor the redox dynamic in cells.

Fluorescent Responses of Probe 1 to SO_2. For sulfite detection, as we designed, the addition of Na_2SO_3 into a system of probe **1** in PBS/DMSO (1/1, v/v, pH 7.4) induced a significant fluorescent emission centered at 576 nm with excitation at 510 nm and peaked with 4-fold enhancement (Figure 2a). Similar to the above-mentioned Cys detection system, the detection process of probe **1** toward Na_2SO_3 (1 equiv probe **1**:20 equiv Na_2SO_3) balanced within 50 s, which indicated that the fluorescence data should be measured 1 min after the addition of analyte (Figure 2b). The detection limit of **1** toward Na_2SO_3 was calculated to be 6.5 μM (Figure 2c). Other analytes, including various amino acids, especially for Cys, Hcy, and GSH, and biological anions, did not interfere with sulfite detection under these condition (Figure 2d). A pH ranging from 4 to 8 was suitable for the detection process (Figure S8). These properties made it possible for **1** to discriminate thiols and sulfite through two emission channels.

Mechanism of Probe 1 Responding to Cys and SO_2. To verify whether the spectroscopic differences in the responses of **1** toward Cys and sulfite were caused by the different sensing mechanisms designed initially, we synthesized a probe−thiols adduct analogue, **1-ME**, and conducted ^1H

DOI: 10.1021/jacs.6b12845
J. Am. Chem. Soc. 2017, 139, 3181−3185

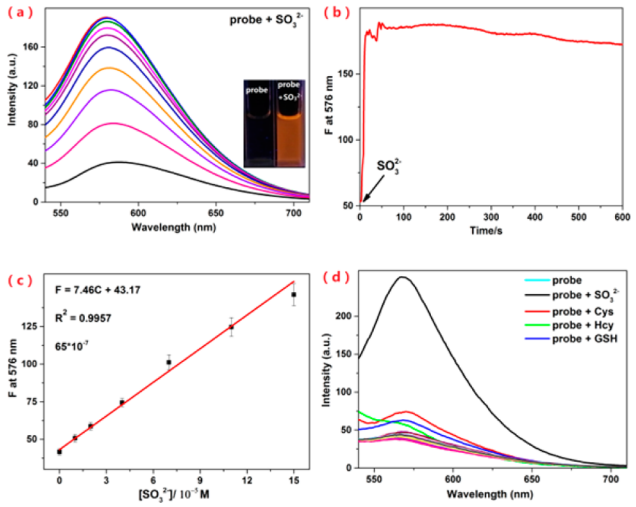

Figure 2. (a) Fluorescent response of 20 μM probe **1** upon addition of 400 μM Na_2SO_3 in PBS/DMSO (1/1, v/v, pH 7.4). Inset: corresponding fluorescent color change under the irradiation of a hand-held UV lamp. (b) Time-dependent fluorescence emission of the 20 μM probe **1** and 400 μM Na_2SO_3 system at 576 nm. (c) Working curve of **1** to detect Na_2SO_3, obtained by addition of various concentrations of Na_2SO_3 (0−150 μM) to 20 μM probe **1**. (d) Fluorescent responses of probe **1** toward 400 μM Cys, Hcy, GSH, Ala, Asn, Arg, Asp, Gln, Glu, His, Lys, Met, Ser, Trp, Tyr, SH^-, F^-, Cl^-, Br^-, SO_4^{2-}, NO_3^-, HPO_4^{2-}, and SO_3^{2-}. λ_{ex} = 510 nm; slit, 5 nm/5 nm.

NMR titration experiments. Comparison of the ^{1}H NMR spectra of **1** and **1-ME** in DMSO-d_6 showed that the original signals at 8.09 and 7.73 ppm, which belong to the α,β-unsaturated ketone protons of **1**, disappeared, and new signals appeared at 4.56, 3.71, and 3.61 ppm (Figure S10). At the same time, the aldehyde hydrogen signal persisted. Further, the fluorescence emission spectra of **1-Cys** and **1-ME** in PBS/DMSO systems are similar (Figure S11). These results demonstrated that −SH-induced fluorescence enhancement was caused by the nucleophilic addition reaction of sulfhydryl toward the α,β-unsaturated ketone in **1**. Furthermore, HR-MS data for the Cys−probe **1** system (Figure S13) supported the aforementioned mechanism. For a Na_2SO_3 detection system, ^{1}H NMR titration experiments following the addition of Na_2SO_3 to the solution of **1** in DMSO-d_6 displayed that the original aldehyde hydrogen signal at 10.04 ppm shifted upfield to 4.99 ppm, which could be attributed to the addition of SO_3^{2-} to the aldehyde group of **1** (Figure S14). HR-MS data for the SO_3^{2-}−probe **1** system further demonstrated the sensing mechanism (Figure S15). These results certified the ability of the probe to detect thiols and SO_3^{2-} through two reaction sites.

Fluorescent Imaging of Thiols and SO_2 in Living Cells. Cytotoxicity experiments demonstrated minimal cytotoxicity of probe **1** toward A549 cells at a concentration of 50 μM (81.4% viability, Figure S16). Application of probe **1** for cellular imaging was then measured using A549 cells. Figure 3a displays that thiol-scavenged A549 cells stained with **1** exhibited no fluorescent emission in both the green and orange channels. However, cells directly stained with **1** showed apparent fluorescent emission in the green channel within 4 min (Figure 3b). Further, exogenous SO_3^{2-} in the thiol-scavenged A549 cells exhibited distinct fluorescent emission in the orange channel after being incubated with **1** for 4 min (Figure 3c). The above data indicate that **1** is cytolemma-permeable and could image the endogenous thiols and exogenous SO_3^{2-} through

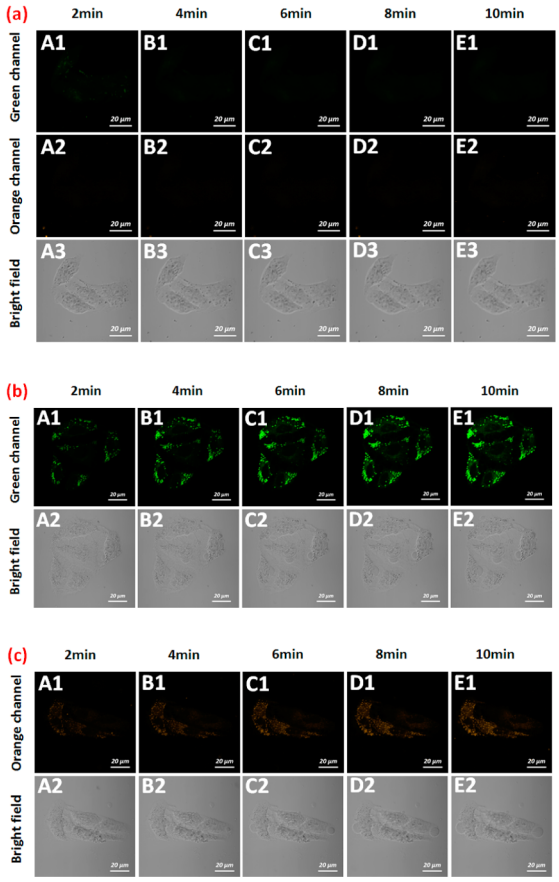

Figure 3. Time-dependent confocal images of endogenous thiols and exogenous SO_3^{2-} in A549 cells. (a) A549 cells pretreated with 1 mM NEM, then incubated with **1** (10 μM). (b) A549 cells incubated with **1** (10 μM). (c) A549 cells pretreated with 1 mM NEM, then incubated with 200 μM Na_2SO_3 for 20 min, and further incubated with **1** (10 μM). Green channel, λ_{em} = 490−520 nm (λ_{ex} = 405 nm); orange channel, λ_{em} = 550−590 nm (λ_{ex} = 514 nm). Scale bar: 20 μm.

two emission channels with high selectivity in living A549 cells. The fast signal output further supports the use of probe **1** for real-time thiols imaging in cells.

Fluorescent Imaging of Cys and SO_2 in Zebrafish. To validate the feasibility of **1** to image Cys and SO_3^{2-} in vivo, we applied **1** in living zebrafish imaging. As shown in Figure 4, NEM-pretreated 5-day-old zebrafish loaded with **1** displayed nearly no fluorescence emission in both the green and orange channels (A1−A3). However, the NEM-pretreated zebrafish further treated with Cys (B1−B3) and SO_3^{2-} (C1−C3) showed significant fluorescent emission after being stained with **1** in the green and orange channels, respectively. D1−D3 displayed that **1** could visualize the distribution of thiols in living zebrafish. These results implied that **1** was tissue-permeable and could detect respectively Cys and SO_3^{2-} through two emission channels in living bodies.

Fluorescent Imaging of H_2O_2-Induced Redox Dynamic in Living Cells. Prompted by the H_2O_2-induced reversibility of the Cys−probe **1** system in vitro, we evaluated the performance of **1** to monitor the redox dynamic in A549 cells stimulated by H_2O_2. Figure 5b,c shows that **1**-loaded A549 cells featured stable fluorescent emission in the green channel within 60 min. However, H_2O_2 incubation of the **1**-loaded A549 cells displayed distinct fluorescent quenching in the following 60 min, especially after 20 min of incubation (Figure 5a,c). This result

DOI: 10.1021/jacs.6b12845
J. Am. Chem. Soc. 2017, 139, 3181−3185

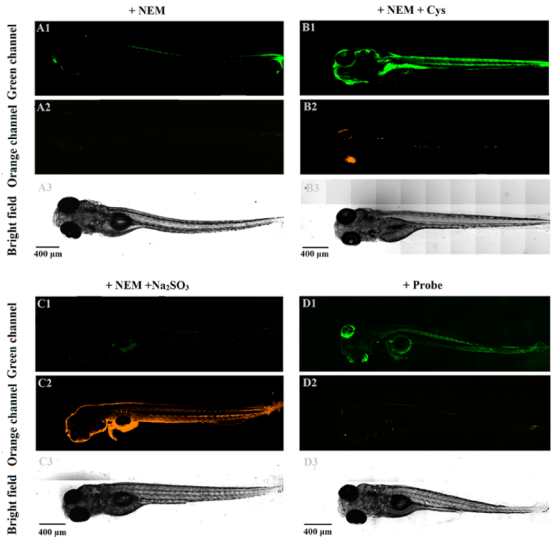

Figure 4. Confocal images of **1** responding to exogenous Cys and SO_3^{2-} and endogenous thiols in 5-day-old zebrafish. (A1−A3) Zebrafish pretreated with NEM (200 μM) for 15 min and then incubated with **1** (10 μM) for 30 min. (B1−B3, C1−C3) Zebrafish pretreated with NEM (200 μM) for 15 min and then incubated with Cys and Na_2SO_3 (100 μM) for 30 min, respectively, and finally incubated with **1** (10 μM) for 30 min. (D1−D3) Zebrafish incubated with **1** (10 μM) for 30 min. From top to bottom: green channel, λ_{em} = 490−520 nm (λ_{ex} = 405 nm); orange channel, λ_{em} = 550−590 nm (λ_{ex} = 488 nm); bright field. Scale bar: 400 μm.

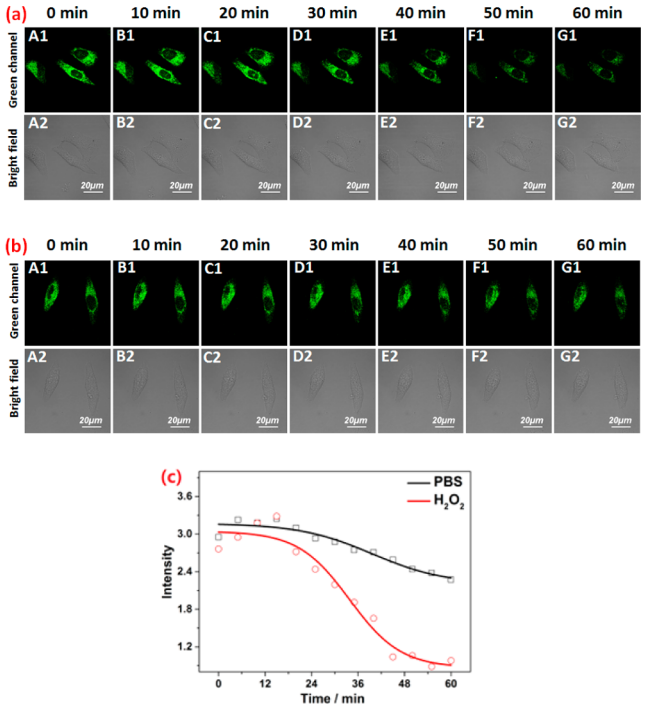

Figure 5. Time-dependent thiols imaging with **1** (10 μM) in A549 cells upon H_2O_2 treatment. (a) A549 cells were pretreated with **1** (10 μM) for 20 min and washed by PBS (10 mM, pH = 7.4) three times, and then H_2O_2 (200 μM) was added. (b) A549 cells were treated with **1** (10 μM) for 20 min and washed by PBS (10 mM, pH = 7.4) three times. Confocal images were then obtained. From top to bottom: green channel, λ_{em} = 490−520 nm (λ_{ex} = 405 nm); bright field. Scale bar: 20 μm. (c) Corresponding time-dependent arithmetic mean intensity changes of the H_2O_2- or PBS-treated cell images.

might be caused by the consumption of H_2O_2 by the originally existing GSH in cells in the initial 20 min, which did not cause apparent fluorescent changes. After equilibrium, **1-Cys** was reduced, and the fluorescent emission was quenched. These results indicated that the probe could image thiols in A549 cells with good photostability and could be used to image the redox dynamic in A549 cells.

Fluorescent Imaging of Cys Metabolism in Living Cells. Supported by the former cellular experiments, we assumed that long-time imaging of Cys-loaded A549 cells might successfully monitor the metabolism of Cys. Thus, we performed time-dependent cell experiments using A549 cells. As shown in Figure 6a, after treatment with 1 mM NEM, 100

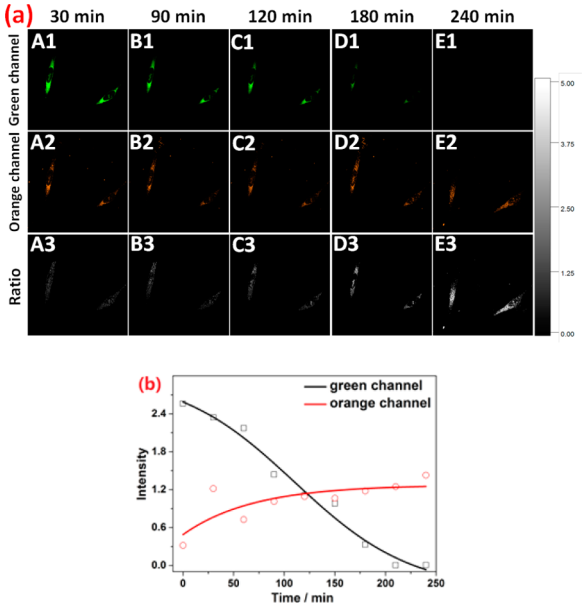

Figure 6. Cys metabolism imaging with **1** (10 μM) in A549 cells. (a) A549 cells incubated with 1 mM NEM for 30 min, 100 μM Cys for 30 min, and 10 μM **1** for 20 min, successively. After washing with PBS, confocal images were obtained. From top to bottom: green channel, λ_{em} = 490−520 nm (λ_{ex} = 405 nm); orange channel, λ_{em} = 550−590 nm (λ_{ex} = 488 nm); ratio images ($R_{O/G}$). (b) Corresponding time-dependent arithmetic mean intensity changes of the obtained images.

μM Cys, and 10 μM **1** successively, the strong fluorescent emission in the green channel quenched gradually in the following 240 min, which reflected the consumption of Cys in cells. Correspondingly, the initial dim fluorescent emission in the orange channel increased, which meant the endogeny of SO_2 (Figure 6b). The ratio images ($R_{O/G}$) established by fluorescence detection of the orange (O) channel and the green (G) channel using Carestream software displayed the concentration changes of Cys and SO_2. The present experiments substantiated that the Cys metabolism produced SO_2 in living A549 cells. Further, as far as we know, this is the first time that fluorescent probes have been used to image the endogenously generated SO_2 without incubation of the SO_2 donors such as $Na_2S_2O_3$ and 2,4-dinitrobenzenesulfonamide.

CONCLUSION

In conclusion, we have developed the first fluorescent probe for visualization of Cys metabolism based on the rational design of dual recognition sites for Cys and its metabolite SO_2, respectively. The probe features fast and reversible fluorescent

DOI: 10.1021/jacs.6b12845
J. Am. Chem. Soc. 2017, 139, 3181−3185

responses toward Cys, which enable the probe to monitor the alterations in Cys concentration induced by NEM and H_2O_2 in vitro. Further, with high selectivity toward thiols and SO_2, the probe was successfully applied for exogenous Cys and SO_2 imaging in zebrafish. Cellular experiments demonstrated that the probe could be used for redox dynamic imaging in A549 cells. Importantly, with ratiometric fluorescent responses, the probe could visualize the enzymatic conversion of Cys to SO_2 in living A549 cells, which provided a deeper insight into the physiological processes of Cys. Supported by the present work, fluorescent probes to image the metabolism of other important thiols are under development in our laboratory, and we believe that these probes will bring a better understanding to the pathological roles of biothiols.

■ ASSOCIATED CONTENT

Supporting Information

The Supporting Information is available free of charge on the ACS Publications website at DOI: 10.1021/jacs.6b12845.

Supplemental figures, synthetic schemes and experimental procedures, and characterization of all compounds (PDF)

■ AUTHOR INFORMATION

Corresponding Authors

*mengxm@ahu.edu.cn

*yincx@sxu.edu.cn

ORCID

Caixia Yin: 0000-0001-5548-6333

Author Contributions

§Y.Y. and F.H. contributed equally.

Notes

The authors declare no competing financial interest.

■ ACKNOWLEDGMENTS

The work was supported by the National Natural Science Foundation of China (Nos. 21472118, 21672131, 21372005), Talents Support Program of Shanxi Province (No. 2014401), and Shanxi Province Outstanding Youth Fund (No. 2014021002).

■ REFERENCES

(1) (a) Ubuka, T.; Ohta, J.; Yao, W. B.; Abe, T.; Teraoka, T.; Kurozumi, Y. *Amino Acids* **1992**, *2* (1−2), 143−55. (b) Du, S. X.; Jin, H. F.; Bu, D. F.; Zhao, X.; Geng, B.; Tang, C. S.; Du, J. B. *Acta Pharmacol. Sin.* **2008**, *29* (8), 923−30. (c) Luo, L.; Chen, S.; Jin, H.; Tang, C.; Du, J. *Biochem. Biophys. Res. Commun.* **2011**, *415* (1), 61−7. (d) Stipanuk, M. H.; Ueki, I. *J. Inherited Metab. Dis.* **2011**, *34* (1), 17−32. (e) Xu, W.; Teoh, C. L.; Peng, J.; Su, D.; Yuan, L.; Chang, Y. T. *Biomaterials* **2015**, *56*, 1−9.

(2) (a) Jung, H. S.; Han, J. H.; Pradhan, T.; Kim, S.; Lee, S. W.; Sessler, J. L.; Kim, T. W.; Kang, C.; Kim, J. S. *Biomaterials* **2012**, *33* (3), 945−53. (b) Jung, H. S.; Pradhan, T.; Han, J. H.; Heo, K. J.; Lee, J. H.; Kang, C.; Kim, J. S. *Biomaterials* **2012**, *33* (33), 8495−502.

(3) (a) Lehmann, A. *Neuroscience* **1987**, *22* (2), 573−578. (b) Heafield, M. T.; Fearn, S.; Steventon, G. B.; Waring, R. H.; Williams, A. C.; Sturman, S. G. *Neurosci. Lett.* **1990**, *110* (1−2), 216−220.

(4) (a) Huo, F. J.; Sun, Y. Q.; Su, J.; Chao, J. B.; Zhi, H. J.; Yin, C. X. *Org. Lett.* **2009**, *11* (21), 4918−21. (b) Niu, L. Y.; Guan, Y. S.; Chen, Y. Z.; Wu, L. Z.; Tung, C. H.; Yang, Q. Z. *Chem. Commun.* **2013**, *49* (13), 1294−6.

(5) (a) Liu, J.; Sun, Y. Q.; Huo, Y.; Zhang, H.; Wang, L.; Zhang, P.; Song, D.; Shi, Y.; Guo, W. *J. Am. Chem. Soc.* **2014**, *136* (2), 574−577. (b) Liu, Y.; Yu, D.; Ding, S.; Xiao, Q.; Guo, J.; Feng, G. *ACS Appl. Mater. Interfaces* **2014**, *6* (20), 17543−50. (c) Yang, X. F.; Huang, Q.; Zhong, Y.; Li, Z.; Li, H.; Lowry, M.; Escobedo, J. O.; Strongin, R. M. *Chem. Sci.* **2014**, *5* (6), 2177−2183. (d) Liu, Y.; Lv, X.; Hou, M.; Shi, Y.; Guo, W. *Anal. Chem.* **2015**, *87* (22), 11475−83. (e) Chen, H.; Tang, Y.; Ren, M.; Lin, W. *Chem. Sci.* **2016**, *7* (3), 1896−1903. (f) Gong, D.; Tian, Y.; Yang, C.; Iqbal, A.; Wang, Z.; Liu, W.; Qin, W.; Zhu, X.; Guo, H. *Biosens. Bioelectron.* **2016**, *85*, 178−83. (g) Kim, C. Y.; Kang, H. J.; Chung, S. J.; Kim, H. K.; Na, S. Y.; Kim, H. J. *Anal. Chem.* **2016**, *88* (14), 7178−82. (h) Zhang, H.; Liu, R.; Liu, J.; Li, L.; Wang, P.; Yao, S. Q.; Xu, Z.; Sun, H. *Chem. Sci.* **2016**, *7* (1), 256−260.

(6) Umezawa, K.; Yoshida, M.; Kamiya, M.; Yamasoba, T.; Urano, Y. *Nat. Chem.* **2016**, DOI: 10.1038/nchem.2648.

(7) (a) Jiang, X.; Yu, Y.; Chen, J.; Zhao, M.; Chen, H.; Song, X.; Matzuk, A. J.; Carroll, S. L.; Tan, X.; Sizovs, A.; Cheng, N.; Wang, M. C.; Wang, J. *ACS Chem. Biol.* **2015**, *10* (3), 864−74. (b) Chen, J.; Jiang, X.; Carroll, S. L.; Huang, J.; Wang, J. *Org. Lett.* **2015**, *17* (24), 5978−81.

(8) (a) Yue, Y. K.; Huo, F. J.; Li, X. Q.; Wen, Y.; Yi, T.; Salamanca, J.; Escobedo, J. O.; Strongin, R. M.; Yin, C. X. *Org. Lett.* **2017**, *19*, 82−85. (b) Yang, J.; Li, K.; Hou, J. T.; Li, L.-L.; Lu, C. Y.; Xie, Y. M.; Wang, X.; Yu, X. Q. *ACS Sensors* **2016**, *1* (2), 166−172. (c) Chen, W.; Fang, Q.; Yang, D.; Zhang, H.; Song, X.; Foley, J. *Anal. Chem.* **2015**, *87* (1), 609−16. (d) Wu, M. Y.; Li, K.; Li, C. Y.; Hou, J. T.; Yu, X. Q. *Chem. Commun.* **2014**, *50* (2), 183−5. (e) Sun, Y. Q.; Liu, J.; Zhang, J.; Yang, T.; Guo, W. *Chem. Commun.* **2013**, *49* (26), 2637−9. (f) Cheng, X.; Jia, H.; Feng, J.; Qin, J.; Li, Z. *J. Mater. Chem. B* **2013**, *1* (33), 4110−4.

(9) (a) Yu, S.; Yang, X.; Shao, Z.; Feng, Y.; Xi, X.; Shao, R.; Guo, Q.; Meng, X. *Sens. Actuators, B* **2016**, *235*, 362−369. (b) Yang, X.-F.; Zhao, M.; Wang, G. *Sens. Actuators, B* **2011**, *152* (1), 8−13. (c) Xie, H.; Zeng, F.; Yu, C.; Wu, S. *Polym. Chem.* **2013**, *4* (21), 5416−5424.

(10) (a) Zhang, Y.; Guan, L.; Yu, H.; Yan, Y.; Du, L.; Liu, Y.; Sun, M.; Huang, D.; Wang, S. *Anal. Chem.* **2016**, *88* (8), 4426−31. (b) Yang, X.; Zhou, Y.; Zhang, X.; Yang, S.; Chen, Y.; Guo, J.; Li, X.; Qing, Z.; Yang, R. *Chem. Commun.* **2016**, *52* (67), 10289−92.

(11) (a) Zhang, Y.; Shao, X.; Wang, Y.; Pan, F.; Kang, R.; Peng, F.; Huang, Z.; Zhang, W.; Zhao, W. *Chem. Commun.* **2015**, *51* (20), 4245−8. (b) Lee, H. Y.; Choi, Y. P.; Kim, S.; Yoon, T.; Guo, Z.; Lee, S.; Swamy, K. M.; Kim, G.; Lee, J. Y.; Shin, I.; Yoon, J. *Chem. Commun.* **2014**, *50* (53), 6967−9. (c) Hong, R.; Han, G.; Fernandez, J. M.; Kim, B. J.; Forbes, N. S.; Rotello, V. M. *J. Am. Chem. Soc.* **2006**, *128* (4), 1078−9.

(12) (a) Hill, J. W.; Coy, R. B.; Lewandowski, P. E. *J. Chem. Educ.* **1990**, *67* (2), 172. (b) Rhee, S. G.; Bae, Y. S.; Lee, S. R.; Kwon, J. *Sci. Signaling* **2000**, *2000* (53), pe1. (c) Luo, D.; Smith, S. W.; Anderson, B. D. *J. Pharm. Sci.* **2005**, *94* (2), 304−16. (d) Gough, D. R.; Cotter, T. G. *Cell Death Dis.* **2011**, *2*, e213. (e) Garcia-Santamarina, S.; Boronat, S.; Hidalgo, E. *Biochemistry* **2014**, *53* (16), 2560−80.

DOI: 10.1021/jacs.6b12845
J. Am. Chem. Soc. 2017, 139, 3181−3185